Chapter 1

Introduction and Overview

1.1 Context of the Present Study

Feasibility Study-II, described here, is a follow-on to Feasibility Study-I [1]. To put our work in context, it is important here to view the effort in a historical perspective, and to give proper credit to our predecessors.

The concept of a Muon Collider was first proposed by Budker [2], and by Skrinsky [3] in the 60s and early 70s. However, there was little substance to the concept until the idea of ionization cooling was developed by Skrinsky and Parkhomchuk [4]. The ionization cooling approach was expanded by Neuffer [5] and then by Palmer [6], whose work led to the formation of the Neutrino Factory and Muon Collider Collaboration (MC) [7] in 1995. A good summary of the Muon Collider concept can be found in the Status Report of 1999 [8]; an earlier document [9], prepared for Snowmass-1996, is also useful reading.

The concept of a Neutrino Factory based on a muon storage ring was suggested by Koshkarev [10], but there was likewise little to the concept until it was combined with the advanced thinking precipitated by the effort toward a Muon Collider. This gap was finally bridged by Geer in 1998 [11].

As a result of this work, the MC realized that a Neutrino Factory could be an important first step toward a Muon Collider. Furthermore, the physics that could be addressed by a Neutrino Factory was interesting in its own right. With this in mind, the MC has recently shifted its primary emphasis toward the issues of relevance to a Neutrino Factory. MUCOOL Notes prepared by the MC are available on the web [12]; these can be used to learn about the technical issues involved. Complementing the Feasibility Studies, the MC carries on an experimental and theoretical R&D program, including work on targetry, cooling, rf hardware (both normal conducting and superconducting), high-field

solenoids, LH_2 absorber design, theory, simulations, parameter studies, and emittance exchange [13]. There is also considerable international activity on Neutrino Factories, with international conferences held at Lyon in 1999, Monterey in 2000, Tsukuba in 2001, and another planned for London in 2002 [14], [15].

In the fall of 1999, Fermilab—with significant contributions from the MC—undertook a Feasibility Study ("Study-I") of an entry-level Neutrino Factory [1]. Simultaneously, Fermilab launched a study of the physics that might be addressed by such a facility [16]. More recently, Fermilab initiated a study to compare the physics reach of a Neutrino Factory with that of conventional neutrino beams [17]; this activity is still in progress. The approach is to examine the physics that can be addressed with a conventional beam, but using an intense proton driver of the type envisioned for the Neutrino Factory, with that physics addressable *only* with a Neutrino Factory. Suffice it to say, there are good physics opportunities in both categories.

It is with this background that the BNL Director, John Marburger, decided in June 2000 to have a follow-on Study on a high-performance Neutrino Factory sited at BNL. Study-II was to be completed by April 2001. Clearly, an important goal of Study-II was to evaluate whether BNL was a suitable site for a Neutrino Factory. Based on the work contained in this report, that question can now be answered affirmatively.

1.2 Expected Performance and Parameters of Major Components

This second Feasibility Study, ("Study II"), commissioned by BNL Director John Marburger, uses BNL site-specific proton driver specifications and a BNL-specific layout of the storage ring, in particular, the pointing angle of the straight sections. It is a follow-up to the FNAL specific ("Study I") study commissioned by the Fermilab Director, that was completed in April 2000 [1] and is site specific in the same spirit, that is, in each study there are a few site-dependent parts; otherwise, the studies are generic. The primary difference is that this study is aimed at a lower muon energy (20 GeV), but higher intensity (for physics reach). Figure 1.1 has been adapted from a figure in the physics study [16]. Both studies were carried out jointly with the Neutrino Factory and Muon Collider Collaboration [18] which has over 140 members from many institutions in the U.S. and abroad.

The design and simulated performance are summarized here; specific details can be found in the chapters that follow.

The efficiency of producing muons at the end of the cooling channel is ≈ 0.17 μ/p

with 24 GeV protons. This higher efficiency translates, per MW of proton beam power, into about 6× that found in Feasibility Study I [1].

The higher efficiency is achieved by:

1. using a liquid mercury target
2. using three induction linacs to achieve nearly non-distorting phase rotation into a longer bunch train with less momentum spread
3. tapering the focusing strength in the cooling system so that the angular spread of the muons being cooled is maintained at a near-constant value
4. increasing the transverse acceptance of the muon acceleration and storage ring.

The components of the system are shown schematically in Fig. 2 (in the Preface).

1.2.1 Components

1.2.1.1 Proton Driver

The proton driver is an upgrade of the Brookhaven Alternating Gradient Synchrotron (AGS) and uses most of the existing components and facilities. The existing booster is replaced by a 1.2 GeV superconducting proton linac. The AGS repetition rate is increased from 0.5 Hz to 2.5 Hz. The total proton charge (10^{14} ppp) is only 40% higher than the current performance of the AGS. The six bunches are extracted separately, spaced by 20 ms, so that the target, induction linacs and rf systems that follow, need only be designed to deal with single bunches at an average repetition rate of 15 Hz, instantaneous rate of 50 Hz. The average power would be 1 MW. A possible future upgrade to 2×10^{14} ppp and 5 Hz could give an average beam power of 4 MW (see, Section B.1). In that scenario, a 1/4 circumference, fixed-field, superconducting bunch compressor ring would be added to reduce the rms bunch length, at the higher intensity, to 3 ns.

1.2.1.2 Target & Capture

A high Z, (mercury) jet target is chosen to give a high yield of pions per incident proton power ($\approx$ 1.9 × that for carbon, which was the choice in Study I).

The jet is continuous, is 1 cm diameter, and enters the target enclosure at a vertical angle of 100 mrad with respect to the magnetic axis. The proton beam intersects the jet at an angle of 33 mrad (*i.e.*, its trajectory is 67 mrad to the magnetic axis). The

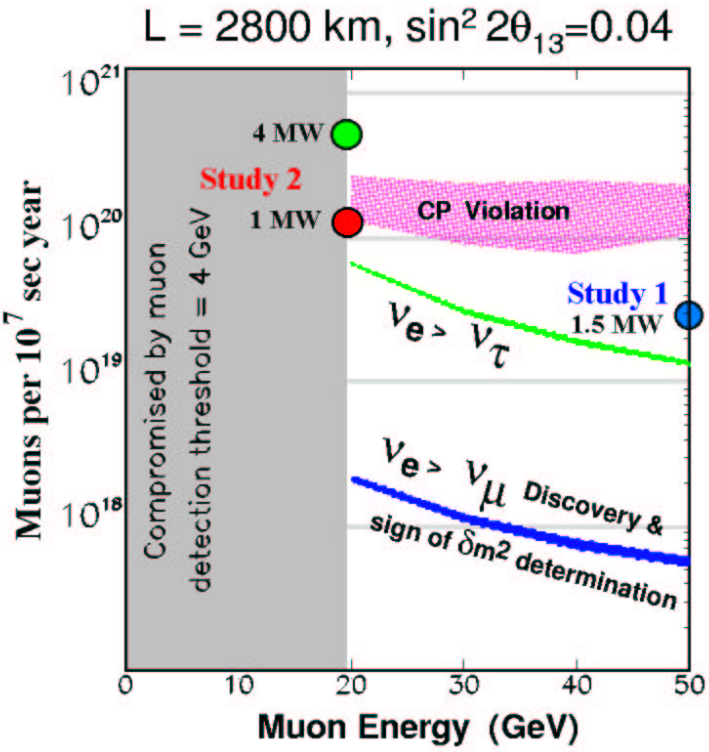

Figure 1.1: Muon decays in a straight section per 10^7 s *vs.* muon energy, with fluxes required for different physics searches assuming a 50 kT detector. Simulated performance of the two studies is indicated.

geometry is shown in Fig. 1.2. It is assumed that the thermal shock from the interacting proton bunch fully disperses the mercury. In this case, the jet must have a velocity of 30 m/s to be replaced before the next bunch. Perturbations to the jet by the capture magnetic field are controlled by placing the jet nozzle inside the field, so that the jet only sees 1 T field changes before it has passed beyond the production region.

Pions emerging from the target are captured and focused down the decay channel by a solenoidal field that is 20 T at the target center, and tapers down, over 18 m, to a periodic (50 cm) superconducting solenoid channel ($< B_z > \approx 1.25$ T) that continues through the phase rotation to the start of bunching.

Figure 1.3 shows a section of the 20 T hybrid magnet, the front end of the taper, the mercury containment, and the mercury pool proton beam dump. The 20 T solenoid,

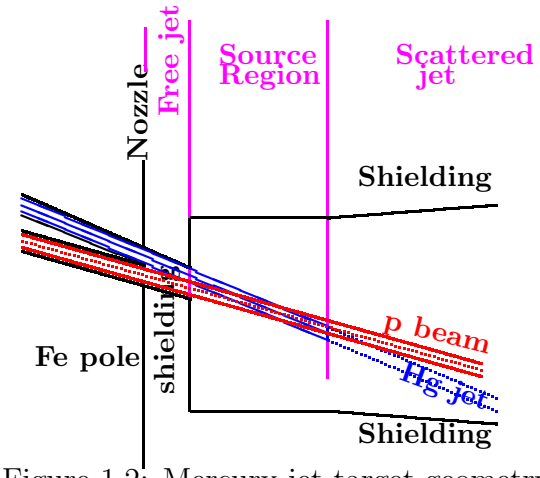

Figure 1.2: Mercury jet target geometry.

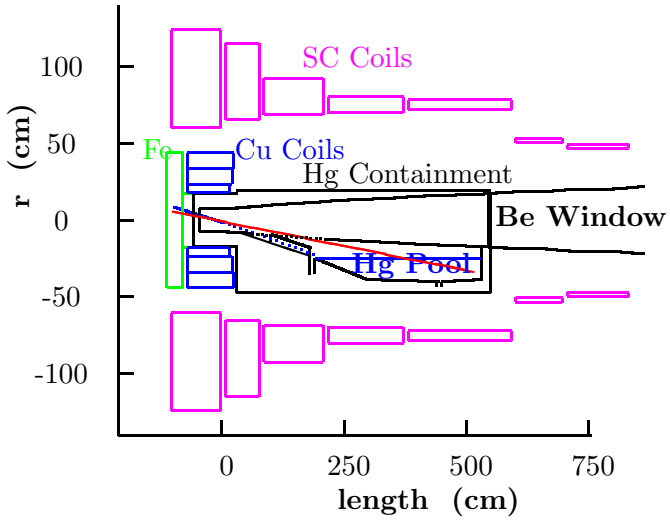

Figure 1.3: Mercury enclosure, mercury-pool beam dump, and solenoid capture magnets.

with a hollow copper conductor magnet insert and superconducting outer coil, is not different in character from the higher field (up to 45 T), but smaller bore, magnets at several existing laboratories. However, the magnet insert in this design is made with hollow copper conductor and ceramic insulation to withstand radiation. MARS [19] simulations of radiation levels show that, with the shielding provided, both copper and superconducting magnets could have a lifetime greater than 20 years, even at 4 MW.

1.2.1.3 Phase Rotation

Pions, and the muons into which they decay, are generated in the target over a very wide range of energies, but in a short time pulse (3 ns rms). This large energy is phase rotated using drifts and induction linacs into a pulse with a longer time duration and a lower energy spread. The muons first drift to spread out their time, the induction linacs then decelerate the early ones and accelerate those later. Three induction linacs (with lengths 100, 80, and 80 m) are used in a system that reduces distortion in the phase-rotated bunch, and allows all induction units to operate with unipolar pulses [20]. The 1.25-T beam transport solenoids are placed inside the induction cores to avoid saturating the core material. The induction units are similar to those being built for DARHT[22].

Between the first and second induction linacs, two hydrogen absorbers (each 1.7 m long and 30 cm radius), with a magnetic field reversal between them, are introduced to reduce the transverse emittance ("minicooling").

1.2.1.4 Buncher

The long bunch (400 ns) after the phase rotation is bunched at 201.25 MHz prior to cooling and acceleration at that frequency. The bunching is done in a lattice identical to that at the start of cooling, and is preceded by a matching section from the 1.25 T solenoids into this lattice. The bunching has three stages, each consisting of rf (with increasing acceleration) followed by drifts with decreasing length (27.5 m, 11 m, 5.5 m). In the first two rf sections, second harmonic rf is used together with the 201.25 MHz to improve the capture efficiency.

1.2.1.5 Cooling

Transverse emittance cooling is achieved by lowering the beam energy in hydrogen absorbers, interspersed with rf acceleration to keep the average energy constant. Transverse and longitudinal momenta are lowered in the absorbers, but only the longitudinal momentum is restored by the rf. The emittance increase from Coulomb scattering is minimized

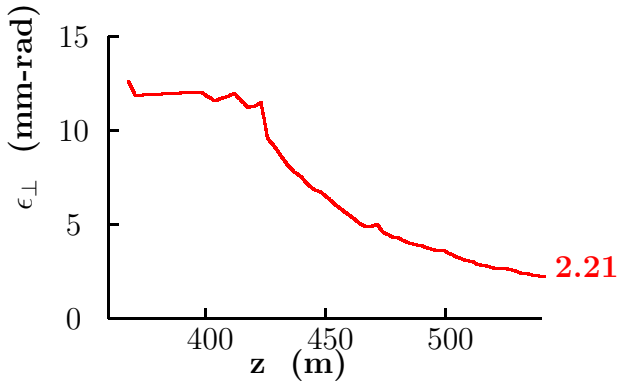

Figure 1.4: Transverse emittance along the cooling channel.

by maintaining the focusing strength so that the angular spread of the beam at the absorber locations is large. This is achieved by keeping the focusing strength inversely proportional to the emittance; *i.e.*, increasing as the emittance is cooled. This could be achieved by a simple solenoid, but such a field also must be reversed periodically to avoid a growth of angular momentum. For this study, a modified Focus-Focus (SFOFO) [21] lattice is employed. The solenoidal fields in each cell alternate in sign and the field shape is chosen to maximize the momentum acceptance (±22%).

Figure 1.4 shows a simulation of cooling, the emittance falls along the length of the channel.

1.2.1.6 Acceleration

A 20 m SFOFO matching section, using normal conducting rf systems, matches the beam optics to the requirements of a 2.5 GeV superconducting rf linac with solenoidal focusing. The linac is in three parts. The first part has a single 2 cavity unit per cell. The second, as a longer period becomes possible, has two 2 cavity units per cell. The last section, with still longer period, accommodates four 2 cavity units per cell.

This linac is followed by a single, recirculating linear accelerator (RLA) that raises the energy from 2.5 GeV to 20 GeV, in 4 passes. This RLA uses the same 4 cavity superconducting structures. The arcs have an average radius of 62 m. The final arc has a dipole field of 2 T.

1.2.1.7 Storage Ring

After acceleration in the RLA, the muons are injected into the upward straight of a racetrack shaped storage ring with a circumference of ≈ 358m. High field superconducting arc magnets are used to minimize the arc length and maximize the fraction (35%) of muons that decay in the downward straight and generate neutrinos headed towards the detector at the WIPP facility in Carlsbad, 2903 km away. All muons are allowed to decay; the total heating from the decay electrons is 42 kW (126 W/m). This load is too high to be dissipated in the superconducting coils. A magnet design has been chosen [23] that allows the majority of these electrons to pass out between separate upper and lower cryostats, and be dissipated in a dump at room temperature. To maintain the vertical cryostat separation in focusing elements, skew quadrupoles are employed in place of standard quadrupoles.

In order to maximize the average bending field, Nb_3Sn pancake coils are employed. One coil of the bending magnet is extended and used as one half of the previous or following skew quadrupole, (see Chapter 7).

Figure 1.5 shows a cross section of the ring, which is kept above the water table and is placed on a roughly 30 m high berm. The 110 m high BNL stack is also shown for scale.

1.2.2 Performance

Complete simulations up to the start of acceleration have been performed using the code MARS [19] (for pion production) followed by ICOOL [24] (for transport, phase rotation and cooling). These results have been confirmed by GEANT4 [25]. They show an average of 0.17 final muons per initial proton on the target, *i.e.*, 0.0071μ/p/GeV, (considering the energy of the initial beam). This can be compared with a value of 0.0011μ/p/GeV produced in Study I [1]. The gain (6×) comes from:

- use of mercury, instead of carbon as a target (1.9 ×)
- use of three, instead of only one, phase rotation induction linacs (2 ×)
- use of a more efficient, tapered cooling channel design (1.4 ×)
- use of a larger accelerator acceptance (1.2 ×)

The muons delivered to the ring with a 1 MW (4 MW) proton driver would be:

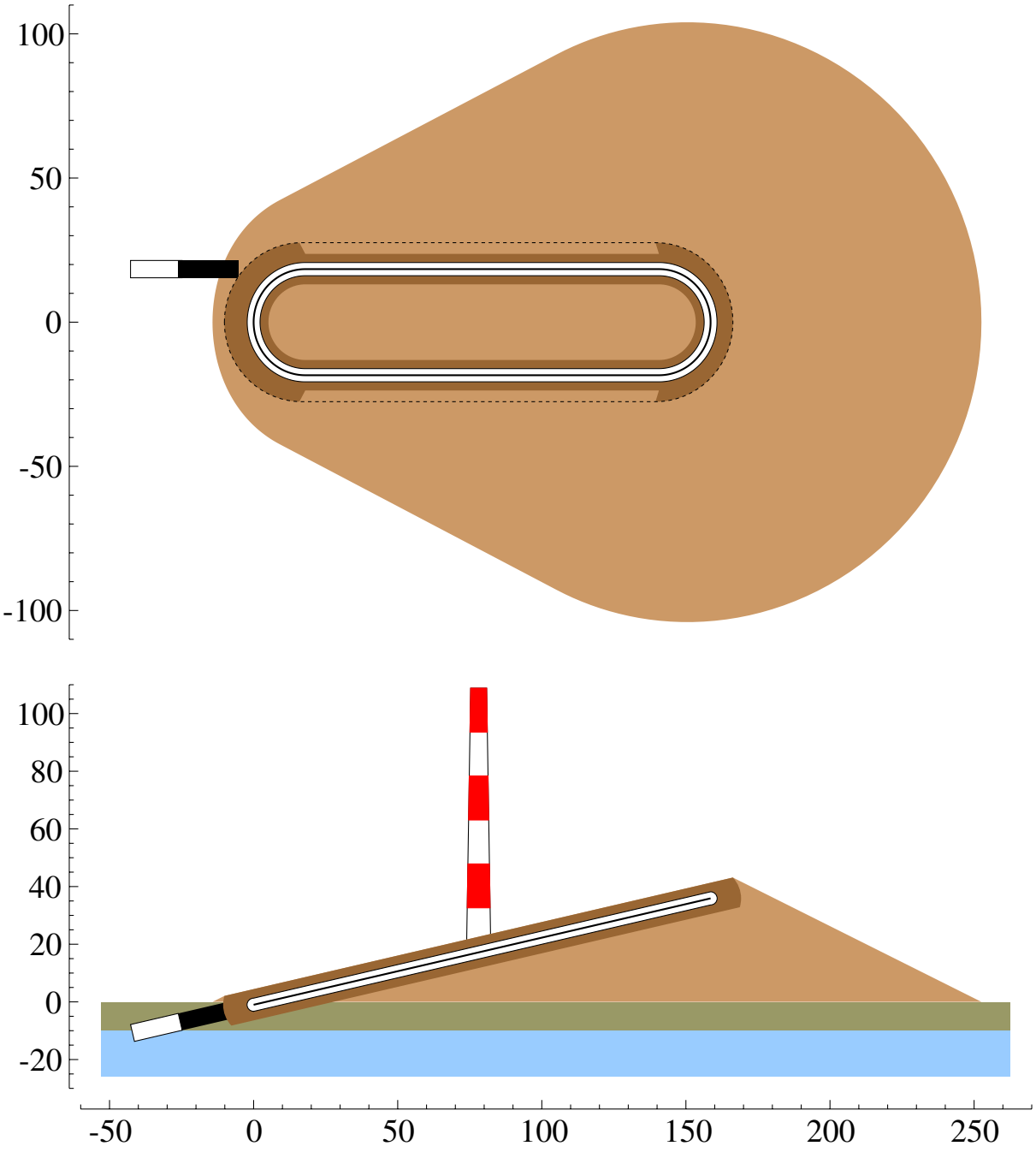

Figure 1.5: Top view and cross section through ring and berm. The 110 m tall tower, drawn to scale, gives a sense of the height of the ring on the BNL landscape.

$$\begin{aligned}\mu/\text{year} &= 10^{14}(\text{ppp}) \times 2.5\ (\text{Hz}) \times 10^{7}\ (\text{s}) \times 0.17\ (\mu/p) \times 0.81\ (\text{acc. efficiency}) \\ &= 3.4 \times 10^{20}\ (= 13.6 \times 10^{20})\end{aligned} \tag{1.1}$$

and the number of muons decaying in the production straight section would be

$$1.2 \times 10^{20}\ \ (=\ 4.8 \times 10^{20})$$

.

1.2.3 Conclusions

This Study II shows significant improvements (6×) over Study-I, yet there remains the possibility of further gains. Cooling of the longitudinal emittance [26] and the capture of both signs [27] appear possible and, together might improve overall performance by a factor between 2 and 4.

1.3 Physics Motivation

Here we discuss the current evidence for neutrino oscillations, and hence neutrino masses and lepton mixing, from solar and atmospheric data. A review is given of some theoretical background including models for neutrino masses and relevant formulas for neutrino oscillation transitions. We next mention the near-term and mid-term experiments in this area and comment on what they hope to measure. We then discuss the physics potential of a muon storage ring as a Neutrino Factory in the long term.

1.3.1 Evidence for Neutrino Oscillations

In a modern theoretical context, one generally expects nonzero neutrino masses and associated lepton mixing. Experimentally, there has been accumulating evidence for such masses and mixing. All solar neutrino experiments (Homestake, Kamiokande, SuperKamiokande (SuperK), SAGE, and GALLEX) show a significant deficit in the neutrino fluxes coming from the Sun [28]. This deficit can be explained by oscillations of the ν_e's into other weak eigenstate(s), with Δm^2_{sol} of the order 10^{-5} eV^2 for solutions involving the Mikheev-Smirnov-Wolfenstein (MSW) resonant matter oscillations [31, 32] or of the order of 10^{-10} eV^2 for vacuum oscillations. Accounting for the data with vacuum oscillations (VO) requires almost maximal mixing. The MSW solutions include one for small mixing angle (SMA) and one with large mixing angle (LMA).

Another piece of evidence for neutrino oscillations is the atmospheric neutrino anomaly, observed by Kamiokande [33], IMB [34], SuperKamiokande [35] with the highest statistics, and also by Soudan [36] and MACRO [37]. These data can be fit by the inference of $\nu_\mu \rightarrow \nu_x$ oscillations with $\Delta m^2_{atm} \sim 3.5 \times 10^{-3}$ eV^2 [35] and maximal mixing, *i.e.*, $\sin^2 2\theta_{atm} = 1$. The identification $\nu_x = \nu_\tau$ is preferred over $\nu_x = \nu_{sterile}$, and the identification $\nu_x = \nu_e$ is excluded by both the SuperKamiokande data and the Chooz experiment [39].

In addition to the above results, the LSND experiment [40] has reported observing $\bar{\nu}_\mu \rightarrow \bar{\nu}_e$ and $\nu_\mu \rightarrow \nu_e$ oscillations with $\Delta m^2_{LSND} \sim 0.1 - 1$ eV^2 and a range of possible mixing angles, depending on Δm^2_{LSND}. This result is not confirmed, but also not completely ruled out, by a similar experiment, KARMEN [41]. The miniBOONE experiment at Fermilab is designed to resolve this issue, as discussed below.

With only three neutrino species, it is not possible to fit all of these experiments. They involve three quite different values of $\Delta m^2_{ij} = m(\nu_i)^2 - m(\nu_j)^2$ which could not satisfy the identity for only three neutrino species that

$$\Delta m^2_{32} + \Delta m^2_{21} + \Delta m^2_{13} = 0. \tag{1.2}$$

It would follow then, that one would have to introduce further neutrino(s). As we know that there are only three leptonic weak doublets, and associated light neutrinos, with weak isospin $T = 1/2$ and $T_3 = 1/2$ from the measurement of the Z width, it follows that additional neutrino weak eigenstates would have to be electroweak singlets (that is, "sterile" neutrinos). Because the LSND experiment has not been confirmed by the KARMEN experiment, we choose here to use only the (confirmed) solar and atmospheric neutrino data in our analysis, and hence to work in the context of three active neutrino weak eigenstates.

1.3.2 Neutrino Oscillation Formalism

In this simplest theoretical context, there are three electroweak-doublet neutrinos. Although electroweak-singlet neutrinos may be present in the theory, one expects that, since their bare mass terms are electroweak-singlet operators, the associated masses should not have any close relation with the electroweak symmetry breaking scale. Indeed, from a top-down point of view, such as a grand unified theory, the masses should be much larger than this scale. If this is the case, then the neutrino mixing can be described by the matrix

$$U = \begin{pmatrix} c_{12}c_{13} & c_{13}s_{12} & s_{13}e^{-i\delta} \\ -c_{23}s_{12} - s_{13}s_{23}c_{12}e^{i\delta} & c_{12}c_{23} - s_{12}s_{13}s_{23}e^{i\delta} & c_{13}s_{23} \\ s_{12}s_{23} - s_{13}c_{12}c_{23}e^{i\delta} & -s_{23}c_{12} - s_{12}c_{23}s_{13}e^{i\delta} & c_{13}c_{23} \end{pmatrix} K' \tag{1.3}$$

where $c_{ij} = \cos\theta_{ij}$, $s_{ij} = \sin\theta_{ij}$, K' is a diagonal matrix with elements $diag(1, e^{i\phi_1}, e^{i\phi_2})$. The phases ϕ_1 and ϕ_2 do not affect neutrino oscillation. Thus, in this framework, the neutrino mixing depends on the four angles θ_{12}, θ_{13}, θ_{23}, and δ, and on two independent differences of squared masses, Δm^2_{atm}, which is $\Delta m^2_{32} = m(\nu_3)^2 - m(\nu_2)^2$ in the favored fit, and Δm^2_{sol}, which may be taken to be $\Delta m^2_{21} = m(\nu_2)^2 - m(\nu_1)^2$. Note that these quantities involve both magnitude and sign; although in a two-species neutrino oscillation in vacuum the sign does not enter, in the three species oscillations relevant here, and including both matter effects and CP violation, the signs of the Δm^2 quantities do enter and can, in principle, be measured.

For our later discussion it will be useful to record the formulas for the various relevant neutrino oscillation transitions. In the absence of any matter effect, the probability that a (relativistic) weak neutrino eigenstate ν_a becomes ν_b after propagating a distance L is

$$\begin{aligned} P(\nu_a \to \nu_b) &= \delta_{ab} - 4\sum_{i>j=1}^{3} Re(K_{ab,ij}) \sin^2\Big(\frac{\Delta m^2_{ij} L}{4E}\Big) \\ &+ 4\sum_{i>j=1}^{3} Im(K_{ab,ij}) \sin\Big(\frac{\Delta m^2_{ij} L}{4E}\Big) \cos\Big(\frac{\Delta m^2_{ij} L}{4E}\Big) \end{aligned} \tag{1.4}$$

where

$$K_{ab,ij} = U_{ai} U^*_{bi} U^*_{aj} U_{bj} \tag{1.5}$$

Note that, in vacuum, CPT invariance implies $P(\bar\nu_b \to \bar\nu_a) = P(\nu_a \to \nu_b)$ and hence, for $b = a$, $P(\bar\nu_a \to \bar\nu_a) = P(\nu_a \to \nu_a)$. For the CP-transformed reaction $\bar\nu_a \to \bar\nu_b$ and the T-reversed reaction $\nu_b \to \nu_a$, the transition probabilities are given by the right-hand side of (1.4) with the sign of the imaginary term reversed. (Below, we shall assume CPT invariance, so that CP violation is equivalent to T violation.)

In most cases there is only one mass scale relevant for long baseline neutrino oscillations, $\Delta m^2_{atm} \sim$ few $\times 10^{-3}$ eV^2 and one possible neutrino mass spectrum is the hierarchical one

$$\Delta m^2_{21} = \Delta m^2_{sol} \ll \Delta m^2_{31} \approx \Delta m^2_{32} = \Delta m^2_{atm} \tag{1.6}$$

In this case, CP (T) violation effects are negligibly small, so that in vacuum

$$P(\bar\nu_a \to \bar\nu_b) = P(\nu_a \to \nu_b) \tag{1.7}$$

$$P(\nu_b \to \nu_a) = P(\nu_a \to \nu_b) \tag{1.8}$$

In the absence of T violation, the second equality Eq. (1.8) would still hold in matter, but even in the absence of CP violation, the first equality Eq. (1.7) would not hold. With the hierarchy (1.6), the expressions for the specific oscillation transitions are

$$\begin{aligned} P(\nu_\mu \to \nu_\tau) &= 4|U_{33}|^2|U_{23}|^2 \sin^2\Big(\frac{\Delta m^2_{atm} L}{4E}\Big) \\ &= \sin^2(2\theta_{23}) \cos^4(\theta_{13}) \sin^2\Big(\frac{\Delta m^2_{atm} L}{4E}\Big) \end{aligned} \tag{1.9}$$

$$\begin{aligned} P(\nu_e \to \nu_\mu) &= 4|U_{13}|^2|U_{23}|^2 \sin^2\Big(\frac{\Delta m^2_{atm} L}{4E}\Big) \\ &= \sin^2(2\theta_{13}) \sin^2(\theta_{23}) \sin^2\Big(\frac{\Delta m^2_{atm} L}{4E}\Big) \end{aligned} \tag{1.10}$$

$$\begin{aligned} P(\nu_e \to \nu_\tau) &= 4|U_{33}|^2|U_{13}|^2 \sin^2\Big(\frac{\Delta m^2_{atm} L}{4E}\Big) \\ &= \sin^2(2\theta_{13}) \cos^2(\theta_{23}) \sin^2\Big(\frac{\Delta m^2_{atm} L}{4E}\Big) \end{aligned} \tag{1.11}$$

In neutrino oscillation searches using reactor antineutrinos, *i.e.*, tests of $\bar\nu_e \to \bar\nu_e$, the two-species mixing hypothesis used to fit the data is

$$\begin{aligned} P(\nu_e \to \nu_e) &= 1 - \sum_x P(\nu_e \to \nu_x) \\ &= 1 - \sin^2(2\theta_{reactor}) \sin^2\Big(\frac{\Delta m^2_{reactor} L}{4E}\Big) \end{aligned} \tag{1.12}$$

where $\Delta m^2_{reactor}$ is the squared mass difference relevant for $\bar\nu_e \to \bar\nu_x$. In particular, in the upper range of values of Δm^2_{atm}, since the transitions $\bar\nu_e \to \bar\nu_\mu$ and $\bar\nu_e \to \bar\nu_\tau$ contribute to $\bar\nu_e$ disappearance, one has

$$P(\nu_e \to \nu_e) = 1 - \sin^2(2\theta_{13}) \sin^2\Big(\frac{\Delta m^2_{atm} L}{4E}\Big) \tag{1.13}$$

i.e., $\theta_{reactor} = \theta_{13}$, and for the value $|\Delta m^2_{atm}| = 3 \times 10^{-3}\text{eV}^2$ from SuperK, the Chooz reactor experiment yields the bound [39]

$$\sin^2(2\theta_{13}) < 0.1 \tag{1.14}$$

which is also consistent with conclusions from the SuperK data analysis [35].

Further, in the three-generation case, the quantity "$\sin^2(2\theta_{atm})$" often used to fit the data on atmospheric neutrinos with a simplified two-species mixing hypothesis, is,

$$\sin^2(2\theta_{atm}) \equiv \sin^2(2\theta_{23})\cos^4(\theta_{13}) \tag{1.15}$$

The SuperK experiment finds that the best fit to their data is to infer $\nu_\mu \to \nu_\tau$ oscillations with maximal mixing, and hence $\sin^2(2\theta_{23}) = 1$ and $|\theta_{13}| << 1$. The various solutions of the solar neutrino problem involve quite different values of Δm^2_{21} and $\sin^2(2\theta_{21})$: (i) large mixing angle solution, LMA: $\Delta m^2_{21} \simeq$ few $\times 10^{-5}$ eV^2 and $\sin^2(2\theta_{21}) \simeq 0.8$; (ii) small mixing angle solution, SMA: $\Delta m^2_{21} \sim 10^{-5}$ and $\sin^2(2\theta_{21}) \sim 10^{-2}$, (iii) LOW: $\Delta m^2_{21} \sim 10^{-7}$, $\sin^2(2\theta_{21}) \sim 1$, and (iv) "just-so": $\Delta m^2_{21} \sim 10^{-10}$, $\sin^2(2\theta_{21}) \sim 1$. The SuperK experiment favors the LMA solution [28]; for other global fits, see, *e.g.*, Gonzalez-Garcia *et al.* in [28].

1.3.3 Types of Neutrino Masses, Seesaw Mechanism

We review here the theoretical background concerning neutrino masses and mixing. In the standard SU(3) $\times$ SU(2)$_L\times$ U(1)$_Y$ model (SM), neutrinos occur in SU(2)$_L$ doublets with $Y = -1$:

$$\mathcal{L}_{L\ell} = \begin{pmatrix} \nu_\ell \\ \ell \end{pmatrix}, \quad \ell = e,\ \mu,\ \tau \tag{1.16}$$

There are no electroweak-singlet neutrinos (often called right-handed neutrinos) $\chi_{R,j}$, $j = 1, ..., n_s$. Equivalently, these could be written as $\overline{\chi^c}_{L,j}$. There are three types of possible Lorentz-invariant bilinear operator products that can be formed from two Weyl fermions ψ_L and χ_R:

- Dirac: $m_D\bar{\psi}_L\chi_R + h.c.$ This connects opposite-chirality fields and conserves fermion number.
- Left-handed Majorana: $m_L\psi_L^T C\psi_L + h.c.$ where $C = i\gamma_2\gamma_0$ is the charge conjugation matrix.
- Right-handed Majorana: $m_R\chi_R^T C\chi_R + h.c.$

The Majorana mass terms connect fermion fields of the same chirality and violate fermion number (by two units). Using the anticommutativity of fermion fields and the property $C^T = -C$, it follows that a Majorana mass matrix appearing as

$$\psi_i^T C(M_{maj})_{ij}\psi_j \tag{1.17}$$

is symmetric in flavor indices:

$$M_{maj}^T = M_{maj} \tag{1.18}$$

Thus, in the Standard Model (SM), there is no Dirac neutrino mass term because: i) it is forbidden as a bare mass term by the gauge invariance; ii) it cannot occur, as do the quark and charged-lepton mass terms, via spontaneous symmetry breaking (SSB) of the electroweak (EW) symmetry starting from a Yukawa term, as there are no EW-singlet neutrinos $\chi_{R,j}$. There is also no left-handed Majorana mass term because: i) it is forbidden as a bare mass term and ii) it would require a Higgs field with $T = 1$, $Y = 2$, but the SM has no such Higgs field. Finally, there is no right-handed Majorana mass term because there is no $\chi_{R,j}$. The same holds for the minimal supersymmetric standard model (MSSM) and the minimal SU(5) grand unified theory (GUT), both for the original and supersymmetric versions.

However, it is easy to add EW-singlet neutrinos χ_R to the SM, MSSM, or SU(5) GUT; these are gauge-singlets under the SM gauge group and SU(5), respectively. Denote these theories as the extended SM, etc. The extended theories give rise to both Dirac and Majorana mass terms, the former via Yukawa terms and the latter as bare mass terms. In the extended SM:

$$-\mathcal{L}_{Yuk} = \sum_{i=1}^{3}\sum_{j=1}^{n_s} h_{ij}^{(D)} \bar{\mathcal{L}}_{L,i}\chi_{R,j}\phi + h.c. \tag{1.19}$$

The electroweak symmetry breaking (EWSB), with

$$\langle\phi\rangle_0 = \begin{pmatrix} 0 \\ v/\sqrt{2} \end{pmatrix} \tag{1.20}$$

where $v = 2^{-1/4}G_F^{-1/2} \simeq 250$ GeV, yields the Dirac mass term

$$\sum_{i=1}^{3}\sum_{j=1}^{n_s} \bar{\nu}_{L,i}(M_D)_{ij}\chi_{Rj} + h.c. \tag{1.21}$$

with

$$(M_D)_{ij} = h_{ij}^{(D)}\frac{v}{\sqrt{2}} \tag{1.22}$$

The Majorana bare mass terms are

$$\sum_{i,j=1}^{n_s} \chi_{Ri}^T C(M_R)_{ij}\chi_{Rj} + h.c. \tag{1.23}$$

For compact notation, define the flavor vectors $\nu = (\nu_e, \nu_\mu, \nu_\tau)$ and $\chi = (\chi_1, .., \chi_{n_s})$ and observe that one can equivalently write ν_L or ν_R^c and χ_R or χ_L^c, where $\psi^c = C\overline{\psi}^T$, $\overline{\psi} = \psi^\dagger\gamma^0$. The full set of Dirac and Majorana mass terms can then be written in the compact matrix form

$$-\mathcal{L}_m = \frac{1}{2}(\bar{\nu}_L \ \overline{\chi^c}_L) \begin{pmatrix} M_L & M_D \\ (M_D)^T & M_R \end{pmatrix} \begin{pmatrix} \nu_R^c \\ \chi_R \end{pmatrix} + h.c. \tag{1.24}$$

where M_L is the 3×3 left-handed Majorana mass matrix, M_R is an $n_s \times n_s$ right-handed Majorana mass matrix, and M_D is the 3-row by n_s-column Dirac mass matrix. In general, all of these are complex, and $(M_L)^T = M_L$, $(M_R)^T = M_R$. Because the extension of the SM to include χ_R does not include a Higgs field with $T = 1$, $Y = 2$, allowing a renormalizable, dimension-4 Yukawa term that would yield a left-handed Majorana mass, one may take $M_L = 0$ at this level (but see below for dimension-5 contributions). The diagonalization of this mass matrix yields the neutrino masses and the corresponding transformation relating the neutrino weak eigenstates to the mass eigenstates.

The same comments apply to the extended MSSM and SU(5) GUT. In the extended SU(5) GUT, the Dirac neutrino mass term arises most simply from the Yukawa couplings of the 5_R with a 5-dimensional Higgs representation H^α (in terms of component fields):

$$\bar{\psi}_{R\alpha} M_D \chi_L^c H^\alpha + h.c. \tag{1.25}$$

and the bare Majorana mass term $\chi_R^T M_R \chi_R + h.c.$.

In the extended SM, MSSM, or SU(5) GUT, one could consider the addition of the χ_R fields as *ad hoc*. However, a more complete grand unification is achieved with the (SUSY) SO(10) GUT, since all of the fermions of a given generation fit into a single representation of SO(10), namely, the 16-dimensional spinor representation ψ_L. In this theory the states χ_R are not *ad hoc* additions, but are guaranteed to exist. In terms of SU(5) representations (recall, SO(10) $\supset$ SU(5) $\times$ U(1))

$$16_L = 10_L + \bar{5}_L + 1_L \tag{1.26}$$

so for each generation, in addition to the usual 15 Weyl fermions comprising the 10_L and 5_R, (equivalently $\bar{5}_L$) of SU(5), there is also an SU(5)-singlet, χ_L^c (equivalently, χ_R). So in SO(10) GUT, electroweak-singlet neutrinos are guaranteed to occur, with number equal to the number of SM generations, inferred to be $n_s = 3$. Furthermore, the generic scale for the coefficients in M_R is expected to be the GUT scale, $M_{GUT} \sim 10^{16}$ GeV.

There is an important mechanism, which originally arose in the context of GUT's, but is more general, that naturally predicts light neutrinos. This is the seesaw mechanism [42].

The basic point is that because the Majorana mass term $\chi_R^T C M_R \chi_R$ is an electroweak singlet, the associated Majorana mass matrix M_R should not be related to the electroweak mass scale v, and from a top-down point of view, it should be much larger than this scale. Denote this generically as m_R. This has the very important consequence that when we diagonalize the joint Dirac-Majorana mass matrix above, the eigenvalues (masses) will be comprised of two different sets: n_s heavy masses, of order m_R, and 3 light masses. We illustrate this in the simplest case of a single generation and $n_s = 1$. Then the mass matrix is simply

$$-\mathcal{L}_m = \frac{1}{2}(\bar{\nu}_L \ \bar{\chi^c}_L) \begin{pmatrix} 0 & m_D \\ m_D & m_R \end{pmatrix} \begin{pmatrix} \nu_R^c \\ \chi_R \end{pmatrix} + h.c. \tag{1.27}$$

The diagonalization yields the eigenvalues

$$\lambda = \frac{1}{2}\left[m_R \pm \sqrt{m_R^2 + 4m_D^2} \right] \tag{1.28}$$

Since $m_D \sim h^{(D)} v$ while m_R is naturally $>> v$ and hence $m_R >> m_D$, we can expand to get

$$\lambda_> \simeq m_R \tag{1.29}$$

and

$$\lambda_< \simeq -\frac{m_D^2}{m_R}\left[1 + O\Big(\frac{m_D^2}{m_R^2}\Big)\right]. \tag{1.30}$$

(The minus sign is not physically important.) The largeness of m_R then naturally explains the smallness of the masses of the known neutrinos. This appealing mechanism also applies in the physical case of three generations and for $n_s \geq 2$.

However, at a phenomenological level, without further theoretical assumptions, there is a large range of values for the light m_ν, since i) the actual scale of m_R is theory-dependent, and ii) it is, *a priori*, not clear what to take for m_D since the known (Dirac) masses range over 5 orders of magnitude, from $m_e, m_u \sim$ MeV to $m_t = 174$ GeV, and this uncertainty gets squared.

For the full case with three generations and $n_s > 1$, and assuming, as is generic, that $det(M_R) \neq 0$ so that M_R^{-1} exists, the set of three light neutrino mass eigenstates is determined by the matrix analogue of eq. (1.30):

$$M_\nu = -M_D M_R^{-1} M_D^T \tag{1.31}$$

A different way to get neutrino masses is to interpret the SM as a low-energy effective field theory, as is common in modern quantum field theory. Provided that their coefficients, of dimension $4 - d_{\mathcal{O}}$ in mass units, are sufficiently small, (nonrenormalizable)

operators $\mathcal{O}$ in the Lagrangian of mass dimension $d_{\mathcal{O}} > 4$, are then allowed. In this case, the dimension-5 operator [43]

$$\mathcal{O} = \frac{1}{M_X} \sum_{a,b} h_{L,ab}(\epsilon_{ik}\epsilon_{jm} + \epsilon_{im}\epsilon_{jk}) \Big[\mathcal{L}^{Ti}_{aL} C \mathcal{L}^{j}_{bL}\Big] \phi^k \phi^m + h.c. \tag{1.32}$$

(where a, b are flavor indices, i, j, k, m are SU(2) indices) is an electroweak singlet. Upon electroweak symmetry breaking (EWSB), this operator yields a left-handed Majorana mass term

$$\sum_{a,b=1}^{3} \nu^T_{L,a} C (M_L)_{ab} \nu_{L,j} + h.c. \tag{1.33}$$

with

$$(M_L)_{ab} = \frac{(h_L)_{ab}(v/\sqrt{2})^2}{M_X} \tag{1.34}$$

Since the SM is phenomenologically very successful, one should have $M_X >> v$, so again these dimension-5 operators lead naturally to light neutrinos. The diagonalization of the above operator determines the unitary transformation relating the mass eigenstates to the weak eigenstates,

$$\nu_{\ell_a} = \sum_{i=1}^{3} U_{ai} \nu_i \ , \quad \ell_1 = e, \ \ell_2 = \mu, \ \ell_3 = \tau \tag{1.35}$$

i.e.,

$$\begin{pmatrix} \nu_e \\ \nu_\mu \\ \nu_\tau \end{pmatrix} = \begin{pmatrix} U_{e1} & U_{e2} & U_{e3} \\ U_{\mu 1} & U_{\mu 2} & U_{\mu 3} \\ U_{\tau 1} & U_{\tau 2} & U_{\tau 3} \end{pmatrix} \begin{pmatrix} \nu_1 \\ \nu_2 \\ \nu_3 \end{pmatrix} \tag{1.36}$$

For the case of electroweak-singlet neutrinos and the resultant seesaw, because of the splitting of the masses into a light set and a heavy set, the observed weak eigenstates of neutrinos are again, to a very good approximation, linear combinations of the three light mass eigenstates, so that the full $(3+n_s)\times(3+n_s)$ mixing matrix breaks into block diagonal form involving the 3×3 U matrix and an analogous $n_s \times n_s$ matrix for the heavy sector. In terms of the flavor vectors, this is

$$\begin{pmatrix} \nu_\ell \\ \chi^c \end{pmatrix} = \begin{pmatrix} U & 0 \\ 0 & U_{heavy} \end{pmatrix} \begin{pmatrix} \nu_i \\ \chi^c_{i,m} \end{pmatrix} \tag{1.37}$$

If all of the data indicating neutrino masses is accepted, including the solar neutrino deficiency, atmospheric neutrinos, and LSND experiments, then light sterile (electroweak-singlet) neutrinos with masses of $\sim$ eV or smaller are needed. These are usually considered

unnatural, because electroweak-singlet neutrinos naturally have masses $\sim m_R >> M_{ew} = v$.

1.3.4 Tests for Neutrino Masses in Decays

Given the focus of this report, we shall not review the well-known kinematic tests for neutrino masses except to mention that these are of three main types. First there are direct tests, which search for the masses of the dominantly coupled neutrino mass eigenstates emitted in particle and nuclear decays; these yield the current upper bounds on these eigenstates for the three dominantly coupled mass components in ν_e, ν_μ, and ν_τ. Second, there are tests for rather massive neutrinos emitted, via lepton mixing, in particle and nuclear decays. Third, there are searches for neutrinoless double beta decay, which would occur if there are massive Majorana neutrinos. The quantity on which limits are put in searches for neutrinoless double beta decay is $\langle m_\nu \rangle = |U_{ei}^2 m(\nu_i)|$ provided that their coefficients, are sufficiently small. Note that since U_{ei} is complex, destructive interference can occur in this sum. At present, the upper limit on this quantity is $\langle m_\nu \rangle \sim 0.4$ eV [44]. A number of new proposals for more sensitive experiments have been put forward, including GENIUS, EXO, MOON, and MAJORANA, among others, which hope to reach a sensitivity below 0.01 eV in $\langle m_\nu \rangle$ [45].

1.3.5 Models for Neutrino Masses and Mixing

We discuss the seesaw mechanism in further detail here. In the SM, a single Higgs field ϕ breaks the gauge symmetry and gives masses to the fermions. In the MSSM, it requires two $T = 1/2$ Higgs fields, H_1 and H_2 with opposite hypercharges $Y = 1$ and $Y = -1$ to do this. GUT theories may have more complicated Higgs sectors; typically different Higgs are used to break the gauge symmetry and give masses to fermions. For the Clebsch-Gordan decomposition of the representations in the fermion mass term we have

$$16 \times 16 = 10_s + 120_a + 126_s \tag{1.38}$$

Hence, *a priori*, one considers using Higgs of dimension 10, 120, and 126. The coupling to the 10-dimensional Higgs fields yields Yukawa terms of the following form (suppressing generation indices).

$$\psi_L^T C \psi_L \bar{\phi}_{10} = (\bar{d}_R d_L + \bar{e}_R e_L)\phi_{10}(\bar{5}) + (\bar{u}_R u_L + \bar{\nu}_R \nu_L)\phi_{10}(5) \tag{1.39}$$

The coupling to the 126-dimensional Higgs yields a term

$$\chi_R^T C \chi_R \phi_{126}(1) \tag{1.40}$$

together with other linear combinations of $\bar{u}_R u_L$, $\bar{\nu}_R \nu_L$, $\bar{d}_R d_L$, and $\bar{e}_R e_L$ times appropriate SU(5)-Higgs; these four types of terms are also produced by the coupling to a 120-dimensional Higgs. Hence, in this approach, one expects some similarity in Yukawa matrices, and thus Dirac mass matrices, for $T_3 = +1/2$ fermions, *i.e.*, the up-type quarks u, c, t and the neutrinos:

$$M^{(u)} \sim M_D^{(\nu)} \ , \quad M^{(d)} \sim M_D^{(\ell)} \tag{1.41}$$

However, in many string-inspired models, high-dimension Higgs representations such as the 120- and 126-dimensional representations in SO(10), are avoided. Instead, one constructs the neutrino mass terms from nonrenormalizable higher-dimension operators. Some reviews of models are in Ref. [46].

To get a rough idea of the predictions, suppose that M_D and M_R are diagonal and let m_R denote a typical entry in M_R. Denote $m_{u,1} = m_u$, $m_{u,2} = m_c$, $m_{u,3} = m_t$. Then, (neglecting physically irrelevant minus signs)

$$m(\nu_i) \simeq \frac{m_{u,i}^2}{m_R} \tag{1.42}$$

This is the quadratic seesaw. For $m(\nu_3)$, one gets

$$m(\nu_3) \sim \frac{m_t^2}{m_R} \simeq \left(\frac{175 \text{ GeV}}{10^{16} \text{ GeV}} \right) (1.75 \times 10^{11} \text{ eV}) \sim 10^{-3} \text{ eV} \tag{1.43}$$

which, given the uncertainties in the inputs, is comparable to the value

$$m(\nu_3) \simeq \sqrt{\Delta m_{32}^2} = \simeq 0.05 \text{ eV} \tag{1.44}$$

inferred from the SuperK data with the assumption $\nu_\mu \to \nu_\tau$ and $m(\nu_2) << m(\nu_3)$. This gives an idea of how the seesaw mechanism could provide a neutrino mass in a region relevant to the SuperKamiokande data.

In passing, we note that string theories allow a low string scale, perhaps as low as 100 TeV. These models have somewhat different phenomenological implications for neutrinos than conventional models with a string scale comparable to the Planck mass.

1.3.6 Lepton Mixing

We proceed to consider off-diagonal structure in M_R, as part of the more general topic of lepton mixing. Neutrino mass terms naturally couple different generations and hence

violate lepton family number; the Majorana mass terms also violate total lepton number. Lepton mixing angles are determined by diagonalizing the charged lepton and neutrino mass matrices, just as the quark mixing angles in the CKM (Cabibbo-Kobayashi-Maskawa) matrix are determined by diagonalizing the up-type and down-type quark mass matrices. Before the atmospheric neutrino anomaly was reported, a common expectation was that lepton mixing angles would be small, like the known quark mixing angles. This was one reason why theorists favored the MSW mechanism over vacuum oscillations as an explanation of the solar neutrino deficiency – MSW could produce the deficiency with small lepton mixing angles, whereas vacuum oscillations needed nearly maximal mixing. It was long recognized that an explanation of the atmospheric neutrino anomaly requires maximal mixing, and while neutrino masses are not surprising or unnatural to most theorists, the maximal mixing has been something of a challenge for theoretical models to explain.

Denoting the lepton flavor vectors as $\ell = (e, \mu, \tau)$ and $\nu = (\nu_e, \nu_\mu, \nu_\tau)$, we have, for the leptonic weak charged current,

$$J^\lambda = \bar{\ell}_L \gamma^\lambda \nu_L \tag{1.45}$$

The mass terms are

$$\bar{\ell}_L M_\ell \ell_R + \bar{\nu}_L M_\nu \nu_R^c + h.c. \tag{1.46}$$

where, as above, $M_\nu = -M_D M_R^{-1} M_D^T$ and we have used the splitting of the neutrino eigenvalues into a light sector and a very heavy sector. We diagonalize these so that, in terms of the associated unitary transformations, with the notation $\ell_m = (e_m, \mu_m, \tau_m)$ and $\nu_m = (\nu_1, \nu_2, \nu_3)$, for charged lepton and neutrino mass eigenstates, the the charged current is

$$J^\lambda = \bar{\nu}_{mL} U_L^{(\nu)} \gamma^\lambda U_L^{(\ell)\dagger} \ell_{mL} = \bar{\nu}_{mL} U \gamma^\lambda \ell_{mL} \tag{1.47}$$

where the lepton mixing matrix is

$$U = U_L^{(\nu)} U_L^{(\ell)\dagger} \tag{1.48}$$

Although many theorists expected before the SuperK results indicating that $\sin^2(2\theta_{23}) = 1$ that leptonic mixing angles would be small, like the quark mixing angles, after being confronted with the SuperK results, they have constructed models that can accommodate large mixing angles. Of course, θ_{13} must be small to fit experiment. Models are able to yield either $\sin^2(2\theta_{12}) \sim 1$ for the LMA, LOW, and just-so solutions, or $\sin^2(2\theta_{12}) << 1$ for the SMA solution.

1.3.7 Relevant Near- and Mid-Term Experiments

There are currently intense efforts to confirm and extend the evidence for neutrino oscillations in all of the various sectors - solar, atmospheric, and accelerator. Some of these experiments are now running. In addition to SuperKamiokande and Soudan-2, these include the Sudbury Neutrino Observatory, SNO, and the K2K long baseline experiment between KEK and Kamioka. Others are in the development and testing phases, such as BOONE, MINOS, the CERN-Gran Sasso (GNGS) program, KAMLAND, and Borexino [47]. Among the long baseline neutrino oscillation experiments, the approximate distances are $L \simeq 250$ km for K2K, 730 km for both MINOS, from Fermilab to Soudan, and the proposed CNGS experiments. K2K is a ν_μ disappearance experiment with a conventional neutrino beam having a mean energy of about 1.4 GeV, going from KEK to the SuperK detector; it has a near detector for beam calibration. It has obtained results consistent with the SuperK experiment, and has reported that its data disagree by 2σ with the no-oscillation hypothesis [38]. MINOS is another conventional neutrino beam experiment that takes a beam from Fermilab to a detector in the Soudan mine in Minnesota. It too uses a near detector for beam flux measurements and has opted for a low-energy configuration, with the flux peaking at about 3 GeV. This experiment expects to start taking data in early 2004 and, after some years of running, to obtain higher statistics than the K2K experiment and to achieve a sensitivity down to roughly the level $\Delta m^2_{32} \sim 10^{-3}\text{eV}^2$. The CNGS program will come on later, around 2005. It will involve taking a higher energy neutrino beam from CERN to the Gran Sasso deep underground laboratory in Italy. This program will emphasize detection of the τ's produced by the ν_τ's that result from the inferred neutrino oscillation transition $\nu_\mu \to \nu_\tau$. The OPERA experiment will do this using emulsions [50], while the ICARUS proposal uses a liquid argon chamber [51]. Moreover, at Fermilab, the MiniBOONE experiment plans to run in the next few years and to confirm or refute the LSND claim after a few years of running.

There are also several relevant solar neutrino experiments. The SNO experiment is currently running and should report their first results in spring 2001. These will involve measurement of the solar neutrino flux and energy distribution using the charged current reaction on heavy water, $\nu_e + d \to e + p + p$. Subsequently, they will measure the neutral current reaction $\nu_e + d \to \nu_e + n + p$. The KamLAND experiment in Japan expects to begin taking data in late 2001. This is a reactor antineutrino experiment using baselines of order 100-250 km and will search for $\bar{\nu}_e$ disappearance. On a similar time scale, the Borexino experiment in Gran Sasso expects to turn on and hopes to measure the ^{7}Be neutrinos from the sun. These experiments should help to decide which of the various solutions to the solar neutrino problem is preferred, and hence the corresponding values of Δm^2_{21} and $\sin^2(2\theta_{12})$.

This, then, is the program of relevant experiments during the period 2001-2010. By the end of this period, we may expect that much will have been learned about neutrino masses and mixing. However, there will remain several important quantities that will not be well measured and which can be measured by a Neutrino Factory.

1.3.8 Oscillation Experiments at a Neutrino Factory

Although a Neutrino Factory based on a muon storage ring will turn on several years after this near-term period in which K2K, MINOS, and the CNGS experiments will run, it has a valuable role to play, given the very high-intensity neutrino beams of fixed flavor-pure content, including, in particular, ν_e and $\bar{\nu}_e$ beams as well as the conventional ν_μ and $\bar{\nu}_\mu$ beams. The potential of the neutrino beams from a muon storage ring is that, in contrast to a conventional neutrino beam, which, say, from π^+ decay, is primarily ν_μ with some admixture of ν_e's and other flavors from K decays, the neutrino beams from the muon storage ring would be extremely high purity: μ^- beams would yield 50 % ν_μ and 50 % $\bar{\nu}_e$, and viceversa for the charge conjugate case of μ^+ beams. Furthermore, these could be produced with extremely high intensities; we shall take the BNL design value of $\approx 10^{20}\mu$ decays per Snowmass year, 10^7 s.

The types of neutrino oscillations that can be explored with the neutrino factory based on a muon storage ring are listed below for the case of μ^- decaying into $\nu_\mu e^- \bar{\nu}_e$:

1. $\nu_\mu \to \nu_\mu$, $\nu_\mu \to \mu^-$ (survival)
2. $\nu_\mu \to \nu_e$, $\nu_e \to e^-$ (appearance)
3. $\nu_\mu \to \nu_\tau$, $\nu_\tau \to \tau^-$; $\tau^- \to (e^-, \mu^-)$... (appearance*)
4. $\bar{\nu}_e \to \bar{\nu}_e$, $\bar{\nu}_e \to e^-$ (survival)
5. $\bar{\nu}_e \to \bar{\nu}_\mu$, $\bar{\nu}_\mu \to \mu^+$ (appearance)
6. $\bar{\nu}_e \to \bar{\nu}_\tau$, $\bar{\nu}_\tau \to \tau^+$; $\tau^+ \to (e^+, \mu^+)$... (appearance*)

where the $*$ on the term appearance refers to the greater difficulty in experimentally inferring the production of the τ particle. It is clear from the list of processes above that, since the beam contains both neutrinos and antineutrinos, the only way to determine the identity of the parent neutrino is to determine the identity of the final-state charged lepton and measure its sign. One aspect of the experiments will involve the measurement of $\nu_\mu \to \nu_\mu$ as a disappearance experiment. A unique aspect for the Neutrino Factory will be the measurement of the oscillation $\bar{\nu}_e \to \bar{\nu}_\mu$, giving a wrong-sign μ^+. Of greater

difficulty would be the measurement of the transition $\bar{\nu}_e \rightarrow \bar{\nu}_\tau$, giving a τ^+ which will decay part of the time to μ^+. These physics goals mean that a detector must have excellent capability to identify muons and measure their charge sign. The oscillation $\nu_\mu \rightarrow \nu_e$ would be difficult to observe, since it would be difficult to identify an electron shower from a hadron shower. From the above formulas for oscillations, we can see that, given the knowledge of $|\Delta m^2_{32}|$ and $\sin^2(2\theta_{23})$ available by the time a Neutrino Factory is built, the measurement of the $\bar{\nu}_e \rightarrow \bar{\nu}_\mu$ transition yields the value of θ_{13}.

To get a rough idea of how the sensitivity of an oscillation experiment would scale with energy and baseline length, recall that the event rate in the absence of oscillations is simply the neutrino flux times the cross section. First of all, neutrino cross sections in the region above about 10 GeV (and slightly higher for τ production) grow linearly with the neutrino energy. Secondly, the beam divergence is a function of the initial muon storage ring energy; this divergence yields a flux, as a function of θ_d, the angle of deviation from the forward direction, that goes like $1/\theta_d^2 \sim E^2$. Combining this with the linear E dependence of the neutrino cross section and the overall $1/L^2$ dependence of the flux far from the production region, one finds that the event rate goes like

$$\frac{dN}{dt} \sim \frac{E^3}{L^2} \tag{1.49}$$

Estimated event rates have been given in the Fermilab Neutrino Factory Working Group Report [16], [17]. For a stored muon energy of 20 GeV, as considered in this report, and a distance of $L = 2900$ to the WIPP Carlsbad site in New Mexico, these event rates amount to several thousand events per kton of detector per year, *i.e.*, they are satisfactory for the physics program. This is also true for the other pathlengths under consideration, namely $L = 2500$ km from BNL to Homestake and $L = 1700$ km to Soudan. A usual racetrack design would only allow a single pathlength L, but a bowtie design could allow two different pathlengths (*e.g.*, [29]).

One could estimate that at a time when the neutrino factory turns on, $|\Delta m^2_{32}|$ and $\sin^2(2\theta_{23})$ would be known at perhaps the 10% level (1 σ) from MINOS [30] (we emphasize that future projections such as this are obviously uncertain and note that JHF anticipates better accuracy; see below). The Neutrino Factory should improve the precision on those two parameters, and can contribute to three important measurements:

- measurement of θ_{13}, as discussed above
- measurement of the sign of Δm^2_{32} using matter effects
- possibly a measurement of CP violation in the leptonic sector, if $\sin^2(2\theta_{13})$, $\sin^2(2\theta_{21})$, and Δm^2_{21} are sufficiently large

It is estimated that a Neutrino Factory with the BNL design parameters could achieve a sensitivity down to $\sin^2 2\theta_{13}) \sim 3 \times 10^{-4}$ or better, assuming a 50 kton water Cherenkov detector at $L = 2900$ km, after three years of running [17, 30]. To measure the sign of Δm^2_{32}, one uses the fact that matter effects reverse sign when one switches from neutrinos to antineutrinos, and carries out this switch in the charges of the stored $\mu^{\pm}$. We elaborate on this next.

1.3.9 Matter Effects

With the advent of the muon storage ring, the distances at which detectors can be placed are large enough that, for the first time, matter effects can be exploited in accelerator-based oscillation experiments. Simply put, matter effects are the matter-induced oscillations that neutrinos undergo along their flight path through the Earth from the source to the detector. Given the typical density of the earth, matter effects are important for the neutrino energy range $E \sim O(10\text{GeV})$ and $\Delta m^2_{32} \sim 10^{-3}$ eV^2, values relevant for the long baseline experiments. After the initial discussion of matter-induced resonant neutrino oscillations in [31], an early study of these effects, including three generations, was carried out in [54]. The sensitivity of an atmospheric neutrino experiment to small Δm^2 due to the long baselines, and the necessity of taking into account matter effects, was discussed *e.g.*, in [55]. After Ref. [32], many analyses were performed in the 1980s of the effects of resonant neutrino oscillations on the solar neutrino flux. Matter effects in the Earth were studied, *e.g.*, [56] and [57], which also discussed the effect on atmospheric neutrinos. Recent papers on matter effects relevant to atmospheric neutrinos include [58, 59]. Early studies of matter effects on long baseline neutrino oscillation experiments were carried out in [60]. More recent analyses relevant to neutrino factories include [52, 53], [61]-[67]. In recent papers [63], calculations were presented of the matter effect for parameters relevant to possible long baseline neutrino experiments envisioned for the Neutrino Factory. In particular, these authors compared the results obtained with constant density along the neutrino path with results obtained by incorporating the actual density profiles. They studied the dependence of the oscillation signal on both $\frac{E}{\Delta m^2_{32}}$ and on the angles in the leptonic mixing matrix, and commented on the influence of Δm^2_{21}.

In the constant-density approximation, one has

$$P(\nu_\mu \to \nu_e) = \sin^2(2\theta^m_{13}) \sin^2\theta_{23} \sin^2(\omega_{32} L) \tag{1.50}$$

where

$$\sin^2(2\theta^m_{13}) = \frac{\sin^2(2\theta_{13})}{\sin^2(2\theta_{13}) + \left[\cos(2\theta_{13}) - \frac{2\sqrt{2} G_F N_e E}{\Delta m^2_{32}}\right]^2} \tag{1.51}$$

and

$$\omega_{32}^2 = \left[\frac{\Delta m_{32}^2}{4E}\sin(2\theta_{13})\right]^2 + \left[\frac{\Delta m_{32}^2}{4E}\cos(2\theta_{13}) - \frac{G_F N_e}{\sqrt{2}}\right]^2 \tag{1.52}$$

where N_e is the electron number density in the medium. For antineutrinos, one reverses the sign of the matter term $\propto G_F N_e$. The resonance condition is that

$$\frac{\Delta m_{32}^2}{2E}\cos(2\theta_{13}) = \sqrt{2} G_F N_e \tag{1.53}$$

i.e., $E \simeq 15$ GeV for $\Delta m_{32}^2 = 3 \times 10^{-3}$ eV^2, $\rho = 3$ g/cm^2, and $Z/A \simeq 0.5$. Thus, if $\Delta m_{32}^2 > 0$, this resonance enhances the $\nu_e \to \nu_\mu$ transition, whereas if $\Delta m_{32}^2 < 0$, it enhances the $\bar{\nu}_e \to \bar{\nu}_\mu$ transition. By comparing these (using first a stored μ^+ beam and then a stored μ^- beam) one can thus determine the sign of Δm_{32}^2 as well as the value of $\sin^2(2\theta_{13})$. A rough estimate is that this could be done to the level $\sin^2(2\theta_{13}) \sim 10^{-3}$.

1.4 CP Violation

CP violation is measured by the (rephasing-invariant) Jarlskog product

$$\begin{aligned} J &= Im(U_{ai} U_{bi}^* U_{aj}^* U_{bj}) \\ &= 2^{-3} \sin(2\theta_{12}) \sin(2\theta_{13}) \cos(\theta_{13}) \sin(2\theta_{23}) \sin\delta \end{aligned} \tag{1.54}$$

Leptonic CP violation also requires that each of the leptons in each charge sector be nondegenerate with any other leptons in this sector; this is, course, true of the charged lepton sector and, for the neutrinos, this requires $\Delta m_{ij}^2 \neq 0$ for each such pair ij. In the quark sector, J is known to be small; $J_{CKM} \sim O(10^{-5})$. A promising asymmetry to measure is $P(\nu_e \to \nu_\mu) - P(\bar{\nu}_e - \bar{\nu}_\mu)$. As an illustration, in the absence of matter effects,

$$\begin{aligned} P(\nu_e \to \nu_\mu) - P(\bar{\nu}_e \to \bar{\nu}_\mu) &= -4J(\sin 2\phi_{32} + \sin 2\phi_{21} + \sin 2\phi_{13}) \\ &= -16 J \sin\phi_{32} \sin\phi_{31} \sin\phi_{21} \end{aligned} \tag{1.55}$$

where

$$\frac{P(\nu_e \to \nu_\mu) - P(\bar{\nu}_e \to \bar{\nu}_\mu)}{P(\nu_e \to \nu_\mu) + P(\bar{\nu}_e \to \bar{\nu}_\mu)} = -\frac{\sin(2\theta_{12}) \cot(\theta_{23}) \sin\delta \sin\phi_{21}}{\sin\theta_{13}} \tag{1.56}$$

In order for the CP violation in Eq. 1.55 to be large enough to measure, it is necessary that θ_{12}, θ_{13}, and $\Delta m_{sol}^2 = \Delta m_{21}^2$ not be too small. From atmospheric neutrino data, we have

$\theta_{23} \simeq \pi/4$ and $\theta_{13} << 1$. If LMA describes solar neutrino data, then $\sin^2(2\theta_{12}) \simeq 0.8$, so $J \simeq 0.1 \sin(2\theta_{13}) \sin\delta$. Say $\sin^2(2\theta_{13}) = 0.04$; then J could be $>> J_{CKM}$. Furthermore, for the upper part of the LMA, $\Delta m^2_{sol} \sim 4 \times 10^{-5}$ eV^2, so the CP violating effects might be observable. In the absence of matter, one would measure the asymmetry

$$\frac{P(\nu_e \to \nu_\mu) - P(\bar{\nu}_e \to \bar{\nu}_\mu)}{P(\nu_e \to \nu_\mu) + P(\bar{\nu}_e \to \bar{\nu}_\mu)} = -\frac{\sin(2\theta_{12}) \cot(\theta_{23}) \sin\delta \sin(2\phi_{21})}{4 \sin(\theta_{13}) \sin^2(\phi_{32})} \tag{1.57}$$

However, in order to optimize this, because of the smallness of Δm^2_{21} even for the LMA, one must go to large pathlengths L, and here matter effects are important. These make leptonic CP violation challenging to measure, because, even in the absence of any intrinsic CP violation, these matter effects render the rates for $\nu_e \to \nu_\mu$ and $\bar{\nu}_e \to \bar{\nu}_\mu$ unequal since the matter interaction is opposite in sign for ν and $\bar{\nu}$. One must therefore subtract out the matter effects in order to try to isolate the intrinsic CP violation. Alternatively, one might think of comparing $\nu_e \to \nu_\mu$ with the time-reversed reaction $\nu_\mu \to \nu_e$. Although this would be equivalent if CPT is valid, as we assume, and although uniform matter effects are the same here, the detector response is quite different and, in particular, it is quite difficult to identify $e^\pm$. Results from SNO and KamLAND testing the LMA will help further planning.

1.4.1 Detector Considerations

We have commented on the requisite properties of detectors. These should be quite massive, O(10-100) kton. Possibilities include magnetized steel calorimetors, water Cherenkov detectors, and liquid-argon chambers. A description of the type of detector presently envisioned for the Neutrino Factory is given in Chapter 15.

1.4.2 Experiments with a High-Intensity Conventional Neutrino Beam

One possibility for the staging of the construction of the neutrino factory is to start with an intense, ~ 1 MW proton driver with an associated program of neutrino physics using a conventional ν_μ neutrino beam from pion decays. Comparisons of the capabilities of a neutrino factory with those of neutrino oscillation experiments with a very high luminosity conventional neutrino beam are discussed in [68]-[69]. The JHF proposal estimates that its planned long baseline $\nu_\mu \to \nu_e$ oscillation experiment to SuperK could reach a level of $\sin^2(2\theta_{13})$ of roughly 10^{-2} [70], and perhaps somewhat better, depending on the type of beam, the running time, and the value of $|\Delta m^2_{32}|$. The recent Fermilab

study reached similar conclusions [30]. The JHF plans also consider the possibility of an upgrade to 4 MW and the construction of a much larger far detector, namely a 1 Mton water Cherenkov detector called HyperKamiokande. Long baseline experiments of this type also intend to carry out $\nu_\mu \to \nu_\mu$ disappearance measurements that will yield much more precise determinations of $\sin^2 2\theta_{23}$ and $|\Delta m^2_{32}|$ than are currently available from the atmospheric data. At Fermilab these plans are being considered in conjunction with plans to construct a more intense proton source [71]. Recently also there have been studies of a number of possible future options, including a 2100 km long baseline experiment using a conventional neutrino beam from JHF to a detector located in the Beijing area [72], an experiment taking a very low energy neutrino beam from CERN to a detector in Frejus [73], and long baseline experiments with a 600 kton water Cherenkov detector called UNO (Ultra Underground Nucleon Decay and Neutrino Detector) [74].

1.4.3 Uses of Intense Low-Energy Muon Beams

The front end of a neutrino factory would be a source of intense low-energy $\mu^\pm$ beams. There is a rich program of physics that could be explored with these beams. Plans are already underway to do this at JHF, using their 3 GeV proton source [75], and at CERN [76], [77]. One of the main areas would be searches for lepton family number violating (LFV) decays, such as $\mu \to e\gamma$ and $\mu \to ee\bar{e}$. A review of the current status of experimental searches for such decays is [78]. The generalization of the standard model to include massive neutrinos and lepton mixing does give rise to these decays, but with branching ratios many orders of magnitude below feasible levels of observation [79]. Models of dynamical electroweak symmetry breaking such as technicolor generically predict large flavor-changing neutral current processes, including these LFV decays. This statement also applies to many types of supersymmetric models [80]. Let us comment on the possible improvements for various decays:

- $\mu \to e\gamma$. A series of experiments of progressively better sensitivity at SIN, TRIUMF, and LASL have been performed to search for this decay. In 1988, the Crystal Box experiment at LASL achieved the limit $B(\mu^+ \to e^+\gamma) < 4.9 \times 10^{-11}$ [81]. This was improved by a factor of 4 by the MEGA experiment at LASL, to $B(\mu^+ \to e^+\gamma) < 1.2 \times 10^{-11}$ [82]. The MEGA experiment took advantage of a stopping μ^+ rate of about 10^8 μ/sec. A proposal has been approved [83] for a $\mu \to e\gamma$ search at PSI with a single event sensitivity of about 10^{-14}. With the increase in the stopping μ decay rate to 10^{13} or more that would be achieved at a low-energy muon facility as part of the neutrino factory, one might envision that it could be possible, if requisite

improvements in background suppression and detector technology could be made, to get to a single event sensitivity of 10^{-15} or better.

- $\mu^+ \to e^+e^+e^-$. The current upper limit on this decay was set by the SINDRUM experiment in 1988 [84]: $B(\mu^+ \to e^+e^+e^-) < 1.0 \times 10^{-12}$. As is the case with $\mu \to e\gamma$, if the necessary background reduction can be achieved and detectors can be designed to take the much greater rates, then with the much higher stopping muon rates at the front end of a neutrino factory, one might be able to reach a sensitivity of 10^{-15} or better in this search.

- $\mu N \to eN$. The current upper limit on muon to electron conversion in the field of a nucleus was set by a PSI experiment [85]: $\sigma(\mu^- + Ti \to e^+ + Ca)/\sigma(\mu^- + Ti \to \nu_\mu + Sc) < 1.7 \times 10^{-12}$. Upgrades of this experiment at PSI hope to reach a sensitivity of $\sim 10^{-13}$. The MECO [86] experiment at Brookhaven plans to search for $\mu + Al \to e + Al$ conversion down to a sensitivity of order $10^{-16} - 10^{-17}$. This is predicated upon obtaining a stopped muon rate of 10^{11} per sec. With the increase in this rate at a neutrino factory to $10^{13} - 10^{14}$ per sec, again if backgrounds can be controlled, one might envision an improvement in the sensitivity of a muon to electron conversion experiment down to the level of perhaps 10^{-18}.

There are also many other interesting experiments that could be pursued. The Brookhaven muon $g-2$ experiment has reported a 2.6 σ discrepancy between the measured value of the anomalous magnetic moment of μ^+ and the theoretical prediction [87, 88]. Further μ^+ data and, in addition, μ^- data, will be analyzed in the near future. The projected sensitivity of this experiment in a_μ is about 0.4×10^{-9}. The current rate of stopping μ's at BNL is about 10^8 per sec. With the increase rate at a neutrino factory, one could perform a higher-statistics version of this experiment. This is particular interest in view of the discrepancy that has been reported between the measured value of the anomalous magnetic moment and the theoretical prediction.

At Brookhaven, a proposal [89] has been submitted for an experiment making use of the existing muon storage ring to search for a muon electric dipole moment (EDM) down to the level of 10^{-22} e-cm in a first stage, with an upgrade having a sensitivity of 10^{-24} e-cm. A more intense source of $\mu^\pm$ would also enable one to push this sensitivity down, perhaps to 10^{-25} e-cm or better.

1.4.4 Conclusions

Neutrino masses and mixing are generic theoretical expectations. The seesaw mechanism naturally yields light neutrinos, although its detailed predictions are model-dependent

and may require a lower mass scale than the GUT mass scale. One of the most interesting findings from the atmospheric data has been the maximal mixing in the relevant channel, which at present is favored to be $\nu_\mu \to \nu_\tau$. Even after the near-term program of experiments by K2K, MINOS, CNGS, and MiniBOONE, a high-intensity Neutrino Factory at BNL with 10^{20} μ decays per Snowmass year and a stored $\mu^\pm$ energy of 20 GeV, coupled with a long-baseline neutrino oscillation experiment, say with $L = 2900$ km to the WIPP facility in Carlsbad, would make a valuable contribution to the physics of neutrino masses and lepton mixing. In particular, the Neutrino Factory should be able to improve the accuracy of the measurement of $\sin^2(2\theta_{23})$ and Δm^2_{32} and to measure $\sin^2(2\theta_{13})$ and the sign of Δm^2_{32}. It might also be able to measure leptonic CP violation.

Bibliography

[1] N. Holtkamp and D. Finley, eds., *A Feasibility Study of a Neutrino Source Based on a Muon Storage Ring*, Fermilab-Pub-00/108-E (2000), http://www.fnal.gov/projects/muon_collider/nu-factory/nu-factory.html

[2] G.I. Budker, in *Proceedings of the 7th International Conf. on High Energy Accelerators*, Yerevan, 1969, p.33; extract in *Physics Potential and Development of $\mu^+\mu^-$ Collidersss: Second Workshop*, Ed. D. Cline, AIP Conf. Proc. **352** (AIP, New York, 1996), p.4.

[3] A.N Skrinsky, *Proceedings of the International Seminar on Prospects of High-Energy Physics*, Morges, 1971 (unpublished);extract in *Physics Potential and Development of $\mu^+\mu^-$ Collidersss: Second Workshop*, Ed. D. Cline, AIP Conf. Proc. **352** (AIP, New York, 1996), p.6.

[4] A.N. Skrinsky and V.V. Parkhomchuk, Sov. J. of Nuclear Physics, 12, 3 (1981).

[5] D. Neuffer, Particle Accelerators, 14, 75 (1983).

[6] R.B. Palmer, D. Neuffer and J. Gallardo, *A practical High-Energy High-Luminosity $\mu^+\mu^-$ Collider*, Advanced Accelerator Concepts: 6th Annual Conference, ed. P. Schoessow, AIP Conf. Proc. **335** (AIP, New York, 1995), p.635; D. Neuffer and R.B. Palmer, *Progress Toward a High-Energy, High-Luminosity $\mu^+\mu^-$ Collider*, The Future of Accelerator Physics: The Tamura Symposium, ed. T. Tajima, AIP Conf. Proc. **356** (AIP, New York, 1996), p.344.

[7] Muon Collaboration Home Page: http://www.cap.bnl.gov/mumu/mu_home_page.html

[8] Charles M. Ankenbrandt *et al.* (Muon Collider Collaboration) Phys. Rev. ST Accel. Beams 2, 081001 (1999) (73 pages), http://publish.aps.org/ejnls/przfetch/abstract/PRZ/V2/E081001/

BIBLIOGRAPHY

[9] *Muon-Muon Collider: A Feasibility Study*, BNL-52503, Fermilab Conf-96/092, LBNL-38946 (1996).

[10] D. Koshkarev, CERN/ ISRDI/7462 (1974).

[11] S. Geer, Phys. Rev. D 57, 6989 (1998).

[12] MUCOOL Notes http://wwwmucool.fnal.gov/notes/notes.html.

[13] MUCOOL home page http://www.fnal.gov/projects/muon_collider/cool/cool.html; Emittance exchange home page http://needmore.physics.indiana.edu/~gail/emittance_exchange.html; Targetry home page http://www.hep.princeton.edu/mumu/target/.

[14] NuFact99, Lyon, http://lyopsr.in2p3.fr/nufact99/.

[15] NuFact00, Monterey, http://www.lbl.gov/Conferences/nufact00/.

[16] C. Albright *et al.*, *Physics at a Neutrino Factory*, Fermilab FN692 (2000) http://www.fnal.gov/projects/muon_collider/nu/study/study.html.

[17] *The Potential for Neutrino Physics at Muon Colliders and Dedicated High Current Muon Storage Rings*, Fermilab (in progress).

[18] J. Gallardo, http://www.cap.bnl.gov/mumu/.

[19] N. Mokhov, http://www-ap.fnal.gov/mars/

[20] R.B. Palmer *Non-Distorting Phase Rotation*, MUC Note 0114, April 2000, (http://www-mucool.fnal.gov/notes/).

[21] Eun-San Kim *et al.*, *LBNL Report on Simulation and Theoretical Studies of Muon Ionization Cooling*, MUC Note 0036, July 1999; Eun-San Kim, M. Yoon, *Super FOFO cooling channel for a Neutrino Factory*, MUC Note 0191, Feb. 2001 (http://www-mucool.fnal.gov/notes/).

[22] M. J. Burns, *et al.*, *DARHT Accelerators Update and Plans for Initial Operation*, Proc. 1999 Acc. Conf., p. 617.

[23] A. Skrinsky, *Towards Ultimate Polarized Muon Collider*, AIP Conf. Proc. 441, 1997, p. 249.

[24] R. Fernow, http://pubweb.bnl.gov/people/fernow/icool/.

[25] The GEANT4 Tool Kit is available at http://wwwinfo.cern.ch/asd/geant4/geant4.html.

[26] G. Hanson, (http://needmore.physics.indiana.edu /g̃ail/emittance_exchange.html).

[27] D. Neuffer, *High Frequency Buncher and $\phi - \delta E$ Rotation for the $\mu^+ - \mu^-$ Source*, MUCOOL Note 0181, Oct. 2000, (http://www-mucool.fnal.gov/notes/).

[28] Fits and references to the Homestake, Kamiokande, GALLEX, SAGE, and Super Kamiokande data include N. Hata and P. Langacker, Phys. Rev. **D56** 6107 (1997); J. Bahcall, P. Krastev, and A. Smirnov, Phys. Rev. **D58**, 096016 (1998); J. Bahcall and P. Krastev, Phys. Lett. **B436**, 243 (1998); J. Bahcall, P. Krastev, and A. Smirnov, Phys. Rev. **D60**, 093001 (1999); J. Bahcall, P. Krastev, and A. Smirnov, hep-ph/0103179; M. Gonzalez-Garcia, C. Peña-Garay, and J. W. F. Valle, Phys. Rev. **D63**, 013007; M. Gonzalez-Garcia, M. Maltoni, C. Pena-Garay, and J. W. F. Valle, Phys. Rev. **D63**, 033005 (2001). Recent discussions of flux calculations are in J. Bahcall, Phys. Rept. **333**, 47 (2000), talk at Neutrino-2000, and http://www.sns.ias.edu/ jnb/. Super Kamiokande data is reported and analyzed in Super Y. Fukuda *et al.* (SuperKamiokande Collab.), Phys. Rev. Lett. **82**, 1810, 243 (1999); S. Fukuda *et al.* (SuperKamiokande Collab.), hep-ex/0103032, hep-ex/0103033. For recent reviews, see e.g., Y. Suzuki, talk at Neutrino-2000, Int'l Conf. on Neutrino Physics and Astrophysics, http://www.nrc.ca/confserv/nu2000/, Y. Takeuchi at ICHEP-2000, Int'l Conf. on High Energy Physics, Osaka, http://ichep2000.hep.sci.osaka-u.ac.jp; and talks at the Fifth Topical Workshop at the Gran Sasso National Laboratory: Solar Neutrinos, Mar., 2001.

[29] Z. Parsa, in Proceedings of NNN99, A.I.P. Conf. Proc. 533, pp. 181-195 (A.I.P., New York, 1999).

[30] V. Barger, R. Bernstein, A. Bueno, M. Campanelli, D. Casper, F. DeJohgh, S. Geer, M. Goodman, D.A. Harris, K.S. McFarland, N. Mokhov, J. Morfin, J. Nelson, F. Peitropaolo, R. Raja, J. Rico, A. Rubbia, H. Schellman, R. Shrock, P. Spentzouris, R. Stefanski, L. Wai, K. Whisnant, FERMILAB-FN-703, hep-ph/0103052.

[31] L. Wolfenstein, Phys. Rev. **D17**, 2369 (1978).

[32] S. P. Mikheyev and A. Smirnov, Yad. Fiz. **42**, 1441 (1985) [Sov.J. Nucl. Phys. **42**, 913 (1986)], Nuovo Cim., **C9**, 17 (1986).

[33] Kamiokande Collab., K. S. Hirata, Phys. Lett. **B205**, 416; *ibid.* **280**, 146 (1992); Y. Fukuda *et al.*, Phys. Lett. **B335**, 237 (1994); S. Hatakeyama *et al.* Phys. Rev. Lett. **81**, 2016 (1998).

[34] IMB Collab., D. Casper *et al.*, Phys. Rev. Lett. **66**, 2561 (1991); R.Becker-Szendy *et al.*, Phys. Rev. **D46**, 3720 (1992); Phys. Rev. Lett. **69**, 1010 (1992).

[35] Y. Fukuda *et al.*, Phys. Lett. **B433**, 9 (1998); Phys. Rev. Lett. **81**,1562 (1998); *ibid.*, **82**, 2644 (1999); Phys. Lett. **B467**, 185 (1999); H. Sobel, in Neutrino-2000, T. Toshito, in ICHEP-2000. Recent discussions of flux calculations are T. Gaisser, Nucl. Phys. (Proc. Suppl.) **87**, 145 (2000); P. Lipari, Astropart. Phys. **14**, 153 (2000); G. Battistoni, hep-ph/0012268; G. Fiorentini, V. Naumov, and F. Villante, hep-ph/0103322.

[36] W. Allison *et al.*, Phys. Lett. **B449**, 137 (1999), A. Mann, talk at Neutrino-2000, hep-ex/0007031.

[37] M. Ambrosio *et al.*, Phys. Lett. **B478**, 5 (2000); B. Barish, talk at Neutrino-2000.

[38] M. Sakuda and K. Nishikawa, talks at ICHEP-2000, Osaka; S. H. Ahn *et al.*, hep-ex/0103001.

[39] M. Apollonio *et al.*, Phys. Lett. **B420**, 397 (1998); Phys. Lett. **B466**, 415 (1999).

[40] LSND Collab., C. Athanassopoulous *et al.*, Phys. Rev. Lett. **77**, 3082 (1996), LSND Collab., C. Athanassopoulous *et al.*, Phys. Rev. Lett. **81**, 1774 (1998); K. Eitel, in Neutrino-2000.

[41] KARMEN Collab., K. Eitel, in Proceedings of Neutrino-2000, Nucl. Phys. (Proc. Suppl.) **91**, 191 (2000).

[42] M. Gell-Mann, P. Ramond, R. Slansky, in *Supergravity*, edited by P. van Nieuwenhuizen and D. Freedman (North Holland, Amsterdam, 1979), p. 315; T. Yanagida in proceedings of *Workshop on Unified Theory and Baryon Number in the Universe*, KEK, 1979.

[43] See, e.g., eq. (1) in R. Shrock, "Neutrinos", in R. Barnett *et al.*, Review of Particle Physics, Phys. Rev. **D54**, 275 (1996).

[44] L. Baudis *et al.*, Phys. Rev. Lett. **83**, 41 (1999); H. Ejiri, in Proceedings of Neutrino 2000, Nucl. Phys. (Proc. Suppl.) **91**, 255 (2000).

[45] E. Fiorini, in in Proceedings of Neutrino 2000, Nucl. Phys. (Proc. Suppl.) **91**, 262 (2000).

[46] There are many reviews of the large number of theoretical models. A few of the recent ones are G. Altarelli and F. Feruglio, hep-ph/9905536, S. Bilenkii, C. Giunti, and W. Grimus, Prog. Part. Nucl. Phys. **43**, 1 (1999); E. Akhmedov, hep-ph/0001264 (ICTP Summer School Lectures, 1999); B. Kayser, A. Smirnov, and R. Mohapatra, in Proc. of Neutrino-2000, Nucl. Phys. B (Proc. Suppl.) **91**, 299, 313 (2000); S. M. Barr, and I. Dorsner, Nucl. Phys. **B585**, 79 (2000); C. H. Albright, hep-ph/0010268; K. Babu, J. Pati, F. Wilczek, Nucl. Phys. **B566**, 33 (2000); P. Ramond, in Proc. of TAUP-99, Nucl. Phys. Proc. Suppl. **87**, 259 (2000), J. Ellis, op cit.

[47] References and websites for these experiments and future projects can be found, e.g., at http://www.hep.anl.gov/ndk/hypertext/nu_industry.html.

[48] Some relevant websites at BNL, FNAL, and CERN containing further information are
http://www.cap.bnl.gov/mumu/
http://www.fnal.gov/projects/muon_collider/nu/study/study.html
http://www.cern.ch/~ autin/nufact99/whitepap.ps
See, in particular, the report of the Fermilab Working Group, C. Albright *et al.*, "FNAL Feasibility Study on a Neutrino Source Based on a Neutrino Storage Ring" (March 30, 2000), available at the above FNAL web site.

[49] Neutrino Factory and Muon Collider Collaboration, Expression of Interest for R+D towards a Neutrino Factory Based on a Storage Ring and Muon Collider, physics/9911009, http://puhep1.princeton.edu/mumu/NSFLetter/nsfmain.ps. This site also contains further references to the relevant literature.

[50] OPERA Collab., CERN-SPSC-97-24, hep-ex/9812015.

[51] ICANOE Collab. F. Cavanna *et al.*, LNGS-P21-99-ADD-1,2, Nov 1999; A. Rubbia, hep-ex/0001052.

[52] S. Geer, Phys. Rev. **D57**, 6989 (1998).

[53] De Rujula, M. B. Gavela, and P. Hernandez, Nucl. Phys. **B547**, 21 (1999).

[54] V. Barger, K. Whisnant, S. Pakvasa, and R. J. N. Phillips, Phys. Rev. **D22**, 2718 (1980); V. Barger, K. Whisnant, and R. J. N. Phillips, Rev. Rev. Lett. **45**, 2084 (1980).

[55] D. Ayres, T. Gaisser, A. K. Mann, and R. Shrock, in *Proceedings of the 1982 DPF Summer Study on Elementary Particles and Future Facilities*, Snowmass, p. 590; D. Ayres, B. Cortez, T. Gaisser, A. K. Mann, R. Shrock, and L. Sulak, Phys. Rev. **D29**, 902 (1984).

[56] P. Krastev, S. Petcov, Phys. Lett. **B205**, 8 (1988).

[57] A. J. Baltz, J. Weneser, Phys. Rev. **D37**, 3364 (1988).

[58] S. Petcov, Phys. Lett. **B434**, 321 (1998). M. Chizhov, M. Maris, S. Petcov, hep-ph/9810501; M. Chizhov, S. Petcov, Phys. Rev. **D63**, 073003 (2001); M.Chizhov, S.Petcov, Phys. Rev. Lett. **83**, 1096 (1999).

[59] E. Akhmedov, A. Dighe, P. Lipari, A. Smirnov, Nucl. Phys. **B542**, 3 (1999); E. Akhmedov, Nucl.Phys. **B538**, 25 (1999); hep-ph/0001264.

[60] P. Krastev, Nuovo Cimento **103A**, 361 (1990); R. H. Bernstein and S. J. Parke, Phys. Rev. **D44**, 2069 (1991).

[61] V. Barger, S. Geer, K. Whisnant, Phys.Rev. **D61**, 053004 (2000).

[62] M. Campanelli, A. Bueno, A. Rubbia, hep-ph/9905240; P. Lipari, Phys. Rev. D61, 113004; D. Dooling, C. Giunti, K. Kang, C. W. Kim, Phys. Rev. **D61** (2000) 073011.

[63] I. Mocioiu, R. Shrock, Phys. Rev. **D62**, 053017 (2000); Proceedings of NNN99, A.I.P. Conf. Proc. 533, pp. 74-79 (A.I.P., New York, 1999).

[64] V. Barger, S. Geer, R. Raja, K. Whisnant, Phys. Rev. **D62**, 013004, *ibid.* **D62**, 073002 (2000); Phys. Lett. —bf B485, 379 (2000); Phys. Rev. **63**, 033002 (2001).

[65] A. Cervera, A. Donini, M.B. Gavela, J. Gomez Cadenas, P. Hernandez, O. Mena, and S. Rigolin, Nucl. Phys. **B579**, 17 (2000), Erratum-ibid. **B593**, 731 (2001).

[66] M. Freund, T. Ohlsson, Mod. Phys. Lett. **15**, 867 (2000); T. Ohlsson, H. Snellman, J. Math. Phys. **41**, 2768 (2000); Phys. Rev. **D60** 093007 (1999); Phys. Lett. **B474**, 153 (2000); M. Freund, M. Lindner, S.T. Petcov, A. Romanino, Nucl. Phys. **B578**, 27 (2000); M. Freund, P. Huber, M. Lindner, Nucl. Phys. **B585**, 105 (2000); M. Freund, M. Lindner, and S. Petcov. Nucl. Instrum. Meth. **A451**, 18 (2000); K. Dick, M. Freund, P. Huber, and M. Lindner, Nucl. Phys. **B588**, 101; Nucl. Phys. —bf B598, 543 (2001).

[67] S.M. Bilenky, C. Giunti, W.Grimus, Phys.Rev.**D58**, 033001 (1998); K. Dick, M. Freund, M. Lindner, A. Romanino, Nucl. Phys. **B562**, 29 (1999); M. Tanimoto, Phys. Lett. **B462**, 115 (1999); A. Donini, M.B. Gavela, P. Hernandez, Nucl. Phys. **B574**, 23 (2000); M. Koike and J. Sato, Phys. Rev. **D61** 073012 (2000); Erratum-ibid. **D62**, 079903 (2000); M. Koike and J. Sato, Phys. Rev. **D62**, 073006 (2000); M. Koike, T. Ota, and J. Sato, hep-ph/0011387; F. Harrison, W.G. Scott, hep-ph/9912435.

[68] B. Richter, hep-ph/0008222.

[69] V. Barger, S. Geer, R. Raja, K. Whisnant, Phys. Rev. **D63**, 113011 (2001) (hep-ph/0012017).

[70] Y. Itoh *et al.* JHF Neutrino Working Group), Letter of Intent: a Long Baseline Neutrino Oscillation Experiment using the JHF 50 GeV Proton Synchroton and the Super-Kamiokande Detector (Feb. 2000); Y. Itoh *et al.*, The JHF-SuperKamiokande Neutrino Project, at http://neutrino.kek.jp/jhfnu.

[71] See http://www-bd.final.gov/pdriver.

[72] N. Okamura *et al.*, hep-ph/0104220; H. Chen *et al.*, hep-ph/0104266.

[73] J. Cadenas *et al.* (CERN Superbeam Working Group), hep-ph/0105297.

[74] See, *e.g.*, D. Harris, talk at UNO workshop (Aug. 2000), R. Shrock, talks at UNO workshop, June, 2001; http://superk.physics.sunysb.edu/uno/.

[75] See working group 2 in in NuFact2001, http://psux1.kek.jp/ nufact01/.

[76] For a recent general review, see J. Ellis, in Neutrino-2000.

[77] J. Ellis, hep-ph/0105265.

[78] Y. Kuno and Y. Okada, Rev. Mod. Phys. **73**, 151 (2001).

[79] S. Petcov, Yad. Fiz. **25**, 641 (1977) [Sov. J. Nucl. Phys. **25**, 340 (1977)]; W. Marciano and A. Sanda, Phys. Lett. **B67**, 303 (1977); B. W. Lee, S. Pakvasa, R. Shrock, and H. Sugawara, Phys. Rev. Lett. **38**, 937 (1977). These decays have also been studied in models with right-handed charged weak currents in T. P. Cheng and L. F. Li, Phys. Rev. Lett. **38**, 381 (1977).

[80] Some early work is L. Hall and M. Suzuki, Nucl. Phys. **B231**, 419 (1984); I-H. Lee, Phys. Lett. **138B**, 121 (1984); Nucl. Phys. **B246**, 120 (1984); recent calculations include R. Barbieri, L. Hall, and A. Strumia, Nucl. Phys. **B449**, 437 (1995); J. Hisano, D. Nomura, Y. Okada, Y. Shimizu, and M. Tanaka, Phys. Rev. **D58**, 116010 (1998).

[81] R. Bolton *et al.*, (Crystal Box Collab.), Phys. Rev. **D38**, 2077 (1988).

[82] M. Brooks *et al.*, (MEGA Collab.), Phys. Rev. Lett. **83**, 1521 (1999).

[83] Barkov *et al.*, PSI Proposal (1999).

[84] U. Bellgardt *et al.*, Nucl. Phys. **B229**, 1 (1988).

[85] J. Kaulard *et al.*, Phys. Lett. **B422** (1998) 334.

[86] MECO Collab., BNL.

[87] H. Brown *et al.* (Muon $g-2$ Collab.), Phys. Rev. Lett. **86**, 2227 (2001).

[88] For recent discussions, see, e.g., A. Czarnecki and W. Marciano, hep-ph/0102122, F. Jegerlehner, hep-ph/0104304; W. Marciano and B. L. Roberts, hep-ph/0105056 and references therein.

[89] Y. Semertzidis *et al.*, BNL Proposal; see also the proceedings of the BNL EDM Workshop (May, 2001), http://www.edm.bnl.gov/Workshop.